

# Surface-Enhanced Resonance Raman Scattering from Copper(II) 5,10,15,20-Tetrakis(1-methyl-4-pyridyl)porphyrin Adsorbed on Aggregated and Nonaggregated Silver Colloids

Marek Procházka,<sup>†,§</sup> Peter Mojžeš,<sup>\*,†,§</sup> Blanka Vlčková,<sup>\*,‡</sup> and Pierre-Yves Turpin<sup>†</sup>

L.P.B.C. (CNRS URA 2056), Université Pierre et Marie Curie, 4 Place Jussieu, Case 138, F-75252 Paris 5, France, and Department of Physical and Macromolecular Chemistry, Faculty of Science, Charles University, Hlavova 2030, CZ-12840 Prague 2, Czech Republic

Received: November 7, 1996; In Final Form: February 5, 1997<sup>®</sup>

Surface-enhanced resonance Raman scattering (SERRS) from copper(II) 5,10,15,20-tetrakis(1-methyl-4-pyridyl)porphyrin (CuTMPyP(4)) adsorbed on a borohydride-reduced silver colloid was studied as a function of CuTMPyP(4) concentration ranging from  $1 \times 10^{-9}$  to  $1 \times 10^{-6}$  M, using the 441.6 nm excitation line of a He–Cd laser. The OH stretching band of bulk water was employed as an internal intensity standard for normalization of the porphyrin SERRS spectra. The surface coverage of Ag colloidal particles by porphyrin molecules as well as the surface plasmon absorption (SPA) and morphology of the Ag colloid/CuTMPyP(4) systems in dependence on the total porphyrin concentration in the systems were investigated and related to the concentration dependence of the SERRS signal. The plots of the intensities of 12 SERRS spectral bands of the  $A_{1g}$  porphyrin modes against the porphyrin concentration are found to be fairly linear for systems with the total porphyrin concentrations  $1 \times 10^{-8}$  to  $2 \times 10^{-7}$  M, in which all porphyrin molecules introduced into the system are adsorbed on isolated Ag colloidal particles and/or small aggregates of ca. 30–70 particles. By contrast, these plots become highly nonlinear and mode-frequency dependent for systems with total porphyrin concentrations  $\geq 3 \times 10^{-7}$  M containing large aggregates of >100 porphyrin-covered Ag colloidal particles as well as fractions of residual nonadsorbed porphyrin molecules. While the former systems are stable for at least one month and provide a highly reproducible SERRS signal, the stability of the latter ones is limited to several hours. Employment of the 441.6 nm excitation coincident with both the Soret band of the porphyrin and the onset of the SPA band of isolated Ag colloidal particles is thus shown to provide a rather unique possibility of obtaining reproducible SERRS spectra with a linear concentration dependence from pico- to nanomolar quantities of a cationic metalloporphyrin adsorbed on nonaggregated and/or weakly aggregated Ag colloidal particles.

## Introduction

Silver colloids have been employed as SERS-active surfaces since the early days of SERS spectroscopy. SERS activity of Ag colloid/adsorbate systems was independently predicted by Moskovits<sup>1</sup> and proved experimentally by Creighton for aggregated Ag colloid/pyridine systems.<sup>2</sup> Nevertheless, SERS spectra were also obtained from molecules adsorbed on nonaggregated Ag colloids.<sup>3–5</sup> SERS excitation profiles of  $1 \times 10^{-2}$  M pyridine and  $2 \times 10^{-2}$  M NaCl adsorbed on nonaggregated Ag colloidal particles (stabilized by EDTA used for the colloid preparation)<sup>3</sup> as well as of CO chemisorbed on Ag colloidal particles isolated in solid matrix<sup>4</sup> were reported and found to match the surface plasmon absorption (SPA) spectrum of the nonaggregated Ag colloidal particles.<sup>3,4</sup> SERS spectra of  $\text{Cl}^-$ ,  $\text{Br}^-$ , and pyridine were also obtained from systems with nonaggregated Ag colloidal particles.<sup>5</sup> In these studies, however, high concentrations of adsorbates were used, and thus the fundamental advantage of SERS spectroscopy, i.e. the high sensitivity, was not obvious. Furthermore, it was shown and explained theoretically that the SERS enhancement factors are substantially higher for Ag colloidal aggregates than for isolated

Ag colloidal particles.<sup>2,6–8</sup> Moreover, the excitation wavelengths routinely employed in SERS measurements (such as the 514.5 nm line of the  $\text{Ar}^+$  laser) do not coincide with the SPA band of isolated Ag colloidal particles and are thus more suitable for excitations of surface plasmon modes localized on Ag colloidal aggregates that are red shifted with respect to the absorption by isolated particles. For this reason, SERS spectral studies are now commonly carried out on aggregated Ag colloid/adsorbate systems<sup>9,10</sup> despite the fact that problems with the stability of the systems and the reproducibility of their SERS spectra occur with some adsorbates.

Aggregation of metal colloids is known to be influenced by the surface potential of the colloid, by the chemical nature and the concentration of the adsorbate, by the temperature, and by the presence of a preaggregating agent.<sup>11,12</sup> In particular, the systematic study of colloidal aggregation<sup>10</sup> has shown that the concentration of the adsorbate (pyridine) in Au colloid/pyridine systems is the most important factor controlling the rate of aggregation of Au colloidal particles as well as the structure of the resulting aggregates.

In this paper, we first demonstrate the effect of varying the CuTMPyP(4) concentration on the *final state* of Ag colloid aggregation in Ag colloid/CuTMPyP(4) systems using UV–vis absorption spectroscopy and transmission electron microscopy (TEM) as probes. We then focus our attention on calculation and experimental determination of the surface

\* To whom correspondence should be addressed.

<sup>†</sup> Université Pierre et Marie Curie.

<sup>‡</sup> Charles University.

<sup>§</sup> Permanent address: Institute of Physics, Charles University, Ke Karlovu 5, CZ-12116 Prague 2, Czech Republic.

<sup>®</sup> Abstract published in *Advance ACS Abstracts*, April 1, 1997.

coverage of Ag colloidal particles by porphyrin molecules. Furthermore, we report SERRS spectra obtained from the Ag colloid/CuTMPyP(4) systems excited by the 441.6 nm line of a He–Cd laser. We demonstrate a new possibility of normalizing the SERRS spectra for a consequent analysis of their concentration dependence. We analyze the plots of the SERRS signal intensity versus porphyrin concentration and compare them with the concentration dependencies of the morphology and the SPA of the Ag colloid/CuTMPyP(4) systems as well as of the surface coverage. Finally, we discuss the results obtained in terms of the SERS-active system constitution and we demonstrate the advantages of SERRS spectral studies with nonaggregated Ag colloidal particles.

## Experimental Section

**Materials.** Analytical grade chemicals and redistilled deionized water were used for all sample preparations.  $\text{NaBH}_4$  (Merck) and  $\text{AgNO}_3$  (Lachema) were employed for the preparation of silver colloids. The copper(II) 5,10,15,20-tetrakis(1-methyl-4-pyridyl)porphyrin (chloride) (CuTMPyP(4)) was prepared according to the procedure published in ref 13. A  $3 \times 10^{-5}$  M stock solution of CuTMPyP(4) in  $2 \times 10^{-2}$  M phosphate buffer (pH = 7.0) was used for preparation of the SERS-active systems.

**Preparation Procedures.** Silver colloid was prepared by reducing  $\text{AgNO}_3$  with  $\text{NaBH}_4$  according to the preparation protocol described in ref 12. The Ag colloid/porphyrin SERS-active systems were prepared by the addition of the appropriate amount of the stock solution of CuTMPyP(4) into 1 mL of the Ag colloid to obtain the desired porphyrin concentrations. The samples were prepared at room temperature (23 °C).

**Instrumentation.** UV–vis absorption spectra were recorded at room temperature using a Perkin Elmer Lambda 12 UV–vis spectrometer. TEM images of grid-deposited Ag colloid and Ag colloid/adsorbate systems were obtained with a JEOL JEM 200 CV transmission electron microscope. The instrumental magnification was 30000 $\times$ . All SERRS spectra were recorded with a Raman spectrometer based on a double monochromator, Ramanor HG2S (Jobin Yvon), equipped with a single-channel detection system (photomultiplier, Ortec NIM modules). Excitation was provided by the 441.6 nm line of a He–Cd laser (Liconix 4050). The average laser power at the sample was 3–4 mW. Spectra were acquired at room temperature from a free liquid surface formed by a capillary force in the longitudinal narrow ( $10 \times 1$  mm) slot carved in the front wall of the quartz cell (sample volume ca. 0.5 mL). A modified  $120^\circ$  scattering geometry was used: the sample cell was turned around its vertical axis so that the incident beam struck the sample surface at ca.  $60^\circ$  with respect to the surface normal, being partly reflected by the sample surface and partly refracted into the sample volume. Since the monochromator optic axis was perpendicular to the incident laser beam (as in the conventional  $90^\circ$  scattering geometry), scattered radiation coming from the impact point at the surface as well as from the sample volume (restricted by the height and width of a monochromator entrance slit) was analyzed. Regularly, two consecutive scans were recorded and compared. No changes attributable to sample photodecomposition and/or colloid sedimentation were observed. Spectra are presented without any smoothing.

## Results and Discussion

**1. SPA and TEM Images of Ag Colloid/CuTMPyP(4) Systems with Varying Porphyrin Concentrations.** Figure 1 shows the SPA spectra of the parent Ag colloid (curve a) and of the Ag colloid/CuTMPyP(4) systems with porphyrin con-

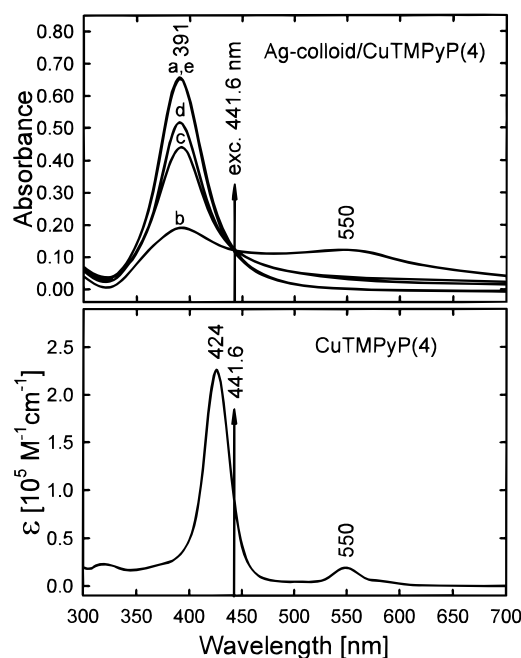


**Figure 1.** SPA spectra of the parent Ag colloid (curve a) and Ag colloid/CuTMPyP(4) systems with a total porphyrin concentration of  $3 \times 10^{-7}$  M (curve b),  $2 \times 10^{-7}$  M (curve c),  $1 \times 10^{-7}$  M (curve d), and  $5 \times 10^{-8}$ ,  $1 \times 10^{-8}$ ,  $5 \times 10^{-9}$ ,  $1 \times 10^{-9}$  M (curve e overlaps with curve a) and electronic absorption spectrum of CuTMPyP(4).

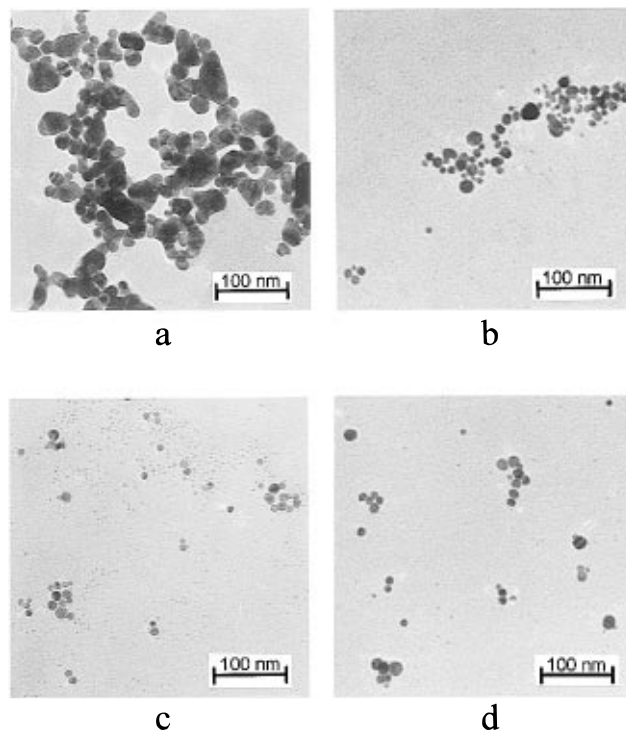


**Figure 2.** TE micrographs of the parent Ag colloid (d) and Ag colloid/CuTMPyP(4) systems with total porphyrin concentrations of  $3 \times 10^{-7}$  M (a),  $1 \times 10^{-7}$  M (b), and  $5 \times 10^{-8}$  M (c).

centrations ranging from  $3 \times 10^{-7}$  to  $1 \times 10^{-9}$  M (curve b–e). Since no distinct electronic absorption bands of CuTMPyP(4) in the spectra b–e are observable, the differences between each of the individual SPA curves b–e and curve a can be interpreted in terms of the varying degree of Ag colloid aggregation as a function of the CuTMPyP(4) concentration. This has been verified by TEM imaging of dried drops of Ag colloid/CuTMPyP(4) systems (Figure 2, micrographs a–c) from which

the SPA curves b, d, and e have been obtained. The TEM image of a dried drop of the parent Ag colloid is shown in Figure 2d.

Additions of porphyrin, providing final concentrations higher than or equal to  $3 \times 10^{-7}$  M, result in a rapid color change of the Ag colloidal solution from yellow to red-orange and finally to blue-gray. The SPA spectrum (Figure 1b) and the TEM image (Figure 2a) of a freshly prepared Ag colloid/CuTMPyP(4) system with a  $3 \times 10^{-7}$  M CuTMPyP(4) concentration indicate a high degree of Ag colloid aggregation.<sup>2,6</sup>

Ag colloid/CuTMPyP(4) systems with the  $1 \times 10^{-7}$  to  $2 \times 10^{-7}$  M final porphyrin concentrations show SPA spectra (Figure 1c,d), the shapes of which differ from that of the parent Ag colloid (Figure 1a) and strongly depend on the actual CuTMPyP(4) concentration. The TEM image of the system with  $1 \times 10^{-7}$  M CuTMPyP(4) concentration (Figure 2b) shows the presence of distinct small aggregates as well as of isolated Ag colloidal particles (sometimes randomly gathered into groups of several particles).

Finally, Ag colloid/CuTMPyP(4) systems with  $1 \times 10^{-9}$  to  $5 \times 10^{-8}$  M porphyrin concentrations provide SPA spectra (Figure 1e) identical to that of the parent Ag colloid (Figure 1a). This indicates that the low concentrations of CuTMPyP(4) were not sufficient to induce aggregation of the Ag colloid. This result is corroborated by the TEM images of the Ag colloid/CuTMPyP(4) ( $5 \times 10^{-8}$  M) system (Figure 2c) and of the parent Ag colloid (Figure 2d). Both TEM images (Figure 2c,d) show isolated Ag colloidal particles (some of which gathered into groups of several particles upon drying of the grid-deposited drop) and are in good agreement with the TEM images of the nonaggregated borohydride-reduced Ag colloid reported by Sánchez-Cortés et al.<sup>14</sup> We thus conclude that in systems with low ( $1 \times 10^{-9}$  to  $5 \times 10^{-8}$  M) CuTMPyP(4) concentrations, the initial, nonaggregated state of Ag colloid remains unchanged.

**2. Determination of the Surface Coverage of Ag Colloidal Particles by CuTMPyP(4) Molecules: Experiment and Calculation.** The concentration dependence of the state of aggregation of Ag colloid/CuTMPyP(4) systems manifests itself also in their stability, as demonstrated by the following experiments. Ag colloid/CuTMPyP(4) systems with the total porphyrin concentrations ranging from  $1 \times 10^{-9}$  to  $1 \times 10^{-5}$  M were stored in the dark at room temperature. While systems with porphyrin concentration  $< 2 \times 10^{-7}$  M remained stable for several weeks, all colloidal particles (aggregates) sedimented from systems with concentration  $\geq 2 \times 10^{-7}$  M within 3 days, as proved spectrophotometrically. Since, for the latter systems, the concentration of the residual, nonadsorbed porphyrin could easily be detected spectrophotometrically, we were able to establish the relationship between the amount of porphyrin molecules introduced into the system and the amount of porphyrin molecules actually adsorbed on Ag colloidal surface. The amount of adsorbed porphyrin molecules was plotted as a function of the total amount (concentration) of the porphyrin molecules present in the system (Figure 3).

The plot in Figure 3 shows that for the porphyrin concentration in the  $(2-3) \times 10^{-7}$  M range almost all porphyrin molecules introduced into the system are adsorbed on the Ag colloidal particles. With a further increase of the porphyrin concentration in the system ( $3 \times 10^{-7}$  to  $1.1 \times 10^{-5}$  M), the amount of the porphyrin molecules adsorbed in 1 mL of the colloid only slowly increases and reaches its saturation value of  $\sim 500 \pm 70$  pmol for a total porphyrin concentration of  $\sim (2-3) \times 10^{-6}$  M.

Furthermore, we calculated the amount of porphyrin molecules required for a monolayer coverage of Ag colloidal particles present in 1 mL of the colloidal system by porphyrin

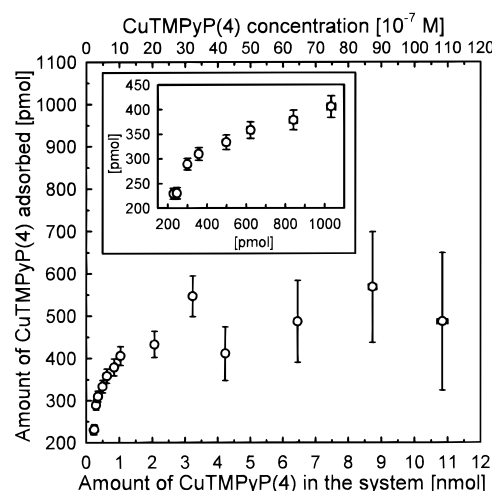


**Figure 3.** The amount of adsorbed CuTMPyP(4) as a function of the total amount (concentration) of CuTMPyP(4) in 1 mL of Ag colloid/CuTMPyP(4).

molecules using the following formula and parameters, assuming, in accord with ref 17, a flat orientation of CuTMPyP(4) with respect to the surface:

$$n = \frac{3FW_{\text{Ag}}}{N_{\text{A}}rS\rho_{\text{Ag}}}VC_{\text{Ag}}$$

where  $FW_{\text{Ag}}$  and  $\rho_{\text{Ag}}$  are the formula weight and density of Ag, respectively,  $C_{\text{Ag}}$  is the molar concentration of Ag in the colloidal solution,  $N_{\text{A}}$  is Avogadro's number,  $r$  is the average radius of the colloidal particles,  $S$  is the surface covered by a single adsorbate molecule, and  $V$  is the sample volume. For the colloid used in the present study ( $C_{\text{Ag}} = 2.36 \times 10^{-4}$  M), the average radius  $r \approx 5.5$  nm was determined from TEM micrographs. Taking into account that the diameter of the CuTMPyP(4) is approximately  $\sim 2.0$  nm (from molecular modeling), and that the neighboring porphyrins are separated due to the adsorbate-adsorbate repulsion, the effective diameter of the CuTMPyP(4) was thus set to  $\sim 2.6$  nm. The calculated amount of porphyrin molecules required for monolayer coverage of the colloidal particles in 1 mL of solution is  $\sim 400$  pmol. This result is in a good agreement with that reported for the same Ag colloid and the structurally related 5,10,15,20-tetrakis-(4-carboxyphenyl)porphyrin in ref 11c.

The upper (saturation) limit of the amount of adsorbed porphyrin determined experimentally (Figure 3) is thus only  $\sim 1.25\times$  higher than the calculated amount of porphyrin molecules required for the monolayer coverage. This result indicates that even at high concentrations of porphyrin in the system that would be sufficient for bi- or multilayer coverage of Ag particles (such as  $2 \times 10^{-6}$  to  $1 \times 10^{-5}$  M) formation of the second layer of adsorbed porphyrin molecules is not favored.

**3. SERRS Spectra of CuTMPyP(4) as a Function of the Overall Porphyrin Concentration in the Ag Colloid/CuTMPyP(4) System.** Raman spectra obtained upon the 441.6 nm excitation from the Ag colloid/CuTMPyP(4) systems in which the overall concentration of CuTMPyP(4) ranged from  $1 \times 10^{-9}$  to  $1 \times 10^{-6}$  M are shown in Figure 4a-h. Since, under the same experimental conditions, resonance Raman spectra of the phosphate-buffer CuTMPyP(4) solutions could only be obtained for porphyrin concentrations higher than  $\sim 5 \times 10^{-6}$  M, all the Raman spectra in Figure 4 are undoubtedly the SERRS spectra of CuTMPyP(4) adsorbed on Ag colloidal particles. Wavenumber values of the SERRS spectral bands of CuTMPyP(4) are identical with those published previously.<sup>15</sup>

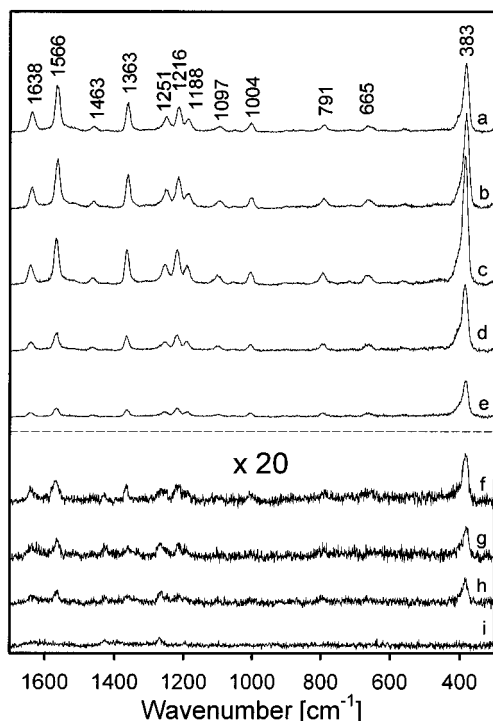


**Figure 4.** SERRS spectra of the Ag colloid/CuTMPyP(4) systems excited by 441.6 nm. Total concentration of CuTMPyP(4): (a)  $1 \times 10^{-6}$  M, (b)  $3 \times 10^{-7}$  M, (c)  $2 \times 10^{-7}$  M, (d)  $1 \times 10^{-7}$  M, (e)  $5 \times 10^{-8}$  M, (f)  $1 \times 10^{-8}$  M, (g)  $5 \times 10^{-9}$  M, (h)  $1 \times 10^{-9}$  M, (i) parent colloid. Spectra a–e and f–h (enlarged 20 $\times$ ) are presented on the identical intensity scales.

The SERRS spectral detection limit of CuTMPyP(4) under the conditions of our experiment (sample volume 0.5 mL) is  $\sim 1$ –2 pmol. The SERRS/RRS enhancement factor roughly estimated from the ratio of concentrations limiting the Raman spectral detection of CuTMPyP(4) by SERRS and by RRS, respectively, is  $\sim 10^3$ , which is in good agreement with the prediction based on the theoretical treatment of the SERRS effect.<sup>16</sup> Furthermore, since we proved that only nonaggregated Ag colloidal particles are present in systems with low ( $1 \times 10^{-9}$  to  $5 \times 10^{-8}$  M) CuTMPyP(4) concentrations, spectra e–h in Figure 4 are the SERRS spectra of CuTMPyP(4) adsorbed on nonaggregated Ag colloidal particles. No SERRS signal from these systems was obtained upon 514.5 nm excitation.

The SERS activity of the Ag colloid/CuTMPyP(4) systems within the wide range of porphyrin concentration ( $10^{-9}$ – $10^{-6}$  M) provides an opportunity to analyze the concentration dependence of SERRS intensity. Such analysis, however, requires a reliable internal intensity standard for normalization of the SERRS spectra. Normal Raman scattering (NRS) of bulk water would be apparently the optimal internal intensity standard for aqueous systems such as Ag-hydrosols. However, water bands are usually too weak to be observed in the SERS spectra excited by the commonly used 514.5 nm excitation. By contrast, our experiments show that, with 441.6 nm excitation, the bands of the OH stretching vibrations of bulk water are clearly observable in the SERRS spectra of Ag colloid/CuTMPyP(4) systems as well as in the NRS spectra of bulk water itself (Figure 5). Furthermore, control experiments carried out under identical experimental conditions (excitation wavelength and energy, laser-spot shape and diameter, geometry of focusing, scattering and signal collecting) indicate that the intensity of the  $3400\text{ cm}^{-1}$  OH stretching band of water retains the same absolute value (deviation  $\leq 10\%$ ) in the Raman spectra obtained from pure water (Figure 5a), from the parent Ag colloid (Figure 5b), and

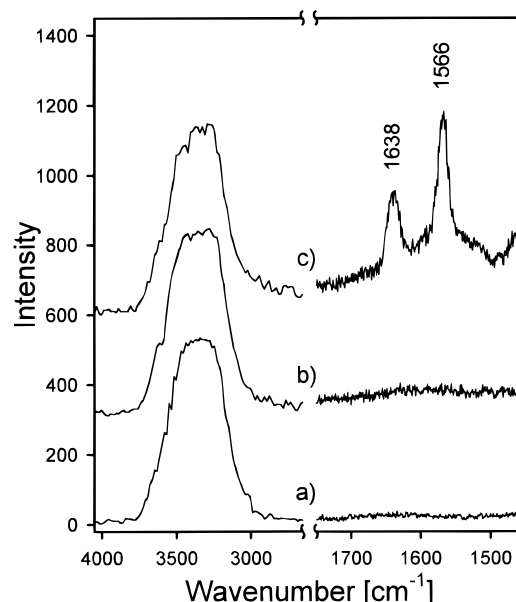


**Figure 5.** Typical Raman spectra of water (a), parent Ag colloid (b), and SERS-active system with  $4 \times 10^{-8}$  M CuTMPyP(4) (c) taken under the identical experimental conditions by 441.6 nm excitation. Spectra are presented in their absolute intensities along with the  $3400\text{ cm}^{-1}$  band of the water OH stretching vibrations.

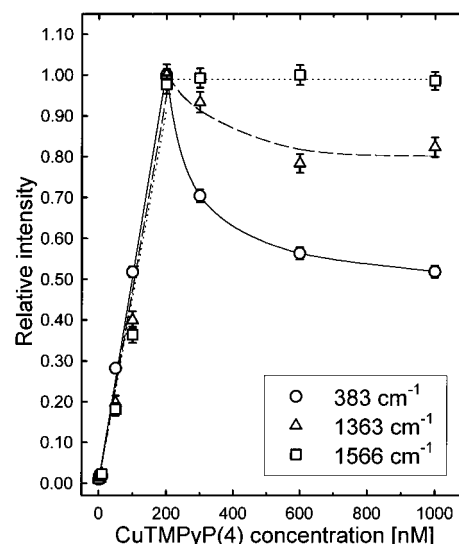


**Figure 6.** Normalized SERRS intensities of the  $383\text{ cm}^{-1}$  ( $\nu_8$ ),  $1363\text{ cm}^{-1}$  ( $\nu_4$ ), and  $1566\text{ cm}^{-1}$  ( $\nu_2$ ) porphyrin bands as a function of the overall CuTMPyP(4) concentration in the Ag colloid/CuTMPyP(4) system.

from the Ag colloid/CuTMPyP(4) system (Figure 5c). The SERRS spectra presented in Figure 4 were thus normalized with respect to the OH stretching band of water.

The normalized intensities of 12 SERRS spectral bands of CuTMPyP(4) (marked in Figure 4) were plotted as a function of the total concentration of CuTMPyP(4) in the Ag colloid/CuTMPyP(4) system. The plots obtained for the  $383\text{ cm}^{-1}$  ( $\nu_8$ ),  $1363\text{ cm}^{-1}$  ( $\nu_4$ ), and  $1566\text{ cm}^{-1}$  ( $\nu_2$ ) bands were selected as typical examples and are presented in Figure 6. For concentrations lower than  $1 \times 10^{-8}$  M, the results are probably affected by rather large errors arising from the adsorption of porphyrin on the glassware and sample cells. In the  $1 \times 10^{-8}$  to  $2 \times 10^{-7}$  M concentration range, all the plots are fairly linear, and the values of slopes of these linear parts show only small mutual differences among the individual plots ( $\alpha \approx (4.94 \pm 0.22) \times 10^{-3}\text{ M}^{-1}$ ), which indicates nearly the same concentration

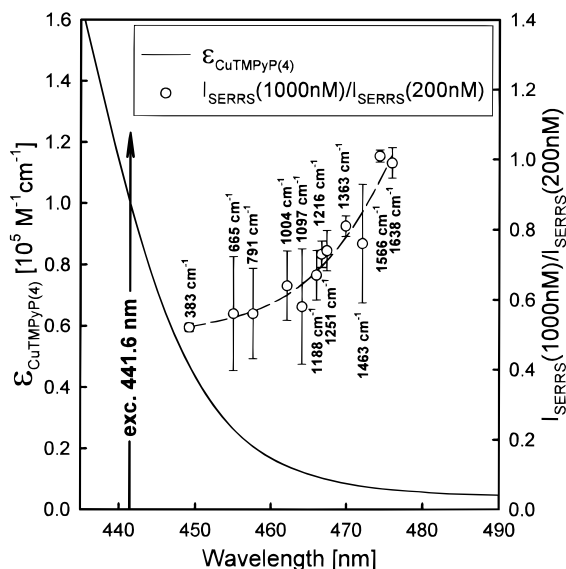


**Figure 7.** Relative decrease of the SERRS signal in the  $2 \times 10^{-7}$  to  $1 \times 10^{-6}$  M concentration range as a function of the vibrational mode frequency (the wavelength of the radiation scattered via the vibrational mode).

dependence of the SERRS intensity for all the CuTMPyP(4) vibrational modes.

For concentration values  $3 \times 10^{-7}$  M and higher, the concentration dependence of the SERRS undergoes a dramatic deviation from the linearly increasing function, providing either a constant (Figure 6c) or a decreasing value of the SERRS signal (Figure 6a,b) with the increase of the CuTMPyP(4) concentration. In this region, the concentration dependence of the SERRS signal differs significantly for the individual Raman bands which, however, all belong to  $A_{1g}$  modes of the porphyrin macrocycle.<sup>18</sup> The magnitude of the decrease of the SERRS signal with the increasing total porphyrin concentration in the system appears to be a function of the mode frequency and, consequently, of the wavelength of the radiation scattered via these vibrational modes. This dependence is demonstrated in detail in Figure 7, in which the decrease of the SERRS signal in the  $1 \times 10^{-8}$  to  $2 \times 10^{-7}$  M range is plotted as a function of the wavelength of the photons scattered via each of the individual porphyrin modes. The same dependence is apparent also from Figure 6, in which the low-frequency  $383 \text{ cm}^{-1}$  mode shows a sharp decrease of the SERRS signal while the intensity of the high-frequency  $1566 \text{ cm}^{-1}$  mode remains constant (Figure 6). The plots of all the other modes fit in between these two extremes (an example being the plot of the  $1363 \text{ cm}^{-1}$  mode), in the order of their increasing frequencies.

Comparison of the plots in Figure 6 with both the micrographs (Figure 2) and the SPA curves of the Ag colloid/CuTMPyP(4) systems (Figure 1) indicates that the linear parts of the concentration dependences were obtained for the systems with CuTMPyP(4) adsorbed on nonaggregated and/or "slightly" aggregated Ag colloidal particles (SPA curves e,d,c in Figure 1 and TEM micrographs b,c in Figure 2). Comparison of micrographs b and c in Figure 2 with the corresponding SPA curves in Figure 1 shows that the difference between the SPA curve of the "slightly" aggregated and the nonaggregated system originates from formation of small aggregates of ca. 30–70 particles in the former case.

By contrast, for the systems with CuTMPyP(4) concentration of  $3 \times 10^{-7}$  M and higher, both the micrograph (Figure 2a) and the SPA curves (Figure 1b) demonstrate formation of large aggregates of more than 100 particles. The concentration dependence of the normalized SERRS intensities of all porphyrin

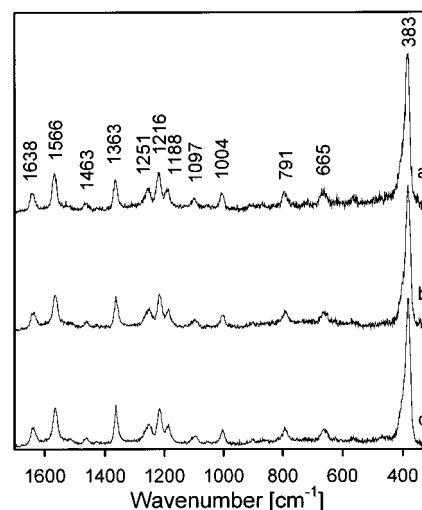


**Figure 8.** Normalized SERRS spectra of  $5 \times 10^{-8}$  M CuTMPyP(4). Spectra a and b were acquired immediately after addition of the porphyrin into colloids from two different samples prepared according to the same procedure. Curve c represents the SERRS spectrum of sample b aged for one month. Spectra are presented on the identical intensity scales.

modes thus undergoes a dramatic change at the same concentration value ( $3 \times 10^{-7}$  M) at which the state of aggregation of Ag colloid has changed from "weak" aggregation (formation of small aggregates of ca. 30–70 particles) to "strong" aggregation (formation of large colloidal aggregates of more than 100 particles).

**4. Linear Part of the Concentration Dependence of the SERRS Intensity: SERRS on Nonaggregated Ag Colloidal Particles.** In the preceding section, we have proved that a fairly linear concentration dependence of the SERRS signal of CuTMPyP(4) is obtained from systems with the porphyrin adsorbed on nonaggregated and/or slightly aggregated Ag colloidal particles. These systems thus appear to be well suited for the quantitative SERRS spectral studies of the CuTMPyP(4) adsorbed on the borohydride-reduced Ag colloid. To support this argument, we tested the reproducibility of the SERRS spectra of CuTMPyP(4) adsorbed on the nonaggregated Ag colloid by the following experiments: First, Ag colloid/CuTMPyP(4) systems with  $5 \times 10^{-8}$  M porphyrin concentration were prepared from two different samples of the colloid obtained by the same preparation procedure.<sup>12</sup> Their SERRS spectra (Figures 8a,b) normalized with respect to the same internal intensity standard as those in Figure 4 (the OH stretching mode of bulk water) are nearly identical. The SERRS spectrum of one of the systems (curve b) was then measured again one month after preparation (Figure 8c) and normalized to the internal intensity standard. The coincidence of curves b and c in Figure 8 demonstrates the reproducibility of the SERRS spectrum as well as the stability of the SERS-active system.

The stability of these systems against aggregation stems from the electrostatic repulsive forces between Ag colloidal particles. We assume that the cationic CuTMPyP(4) porphyrin is adsorbed on Ag colloidal surface negatively charged due to adsorbed ions of the reducing agent ( $\text{BH}_4^-$  and its hydrolytic products, the borates), which are, probably, gradually replaced by  $\text{Cl}^-$  anions introduced into the system as counterions of the porphyrin cation. Our results demonstrate that, in the entire  $1 \times 10^{-8}$  to  $2 \times 10^{-7}$  M concentration range, the electrostatic repulsion barrier between Ag colloidal particles is sufficiently high to prevent "strong aggregation" of Ag colloid, i.e. formation of large colloidal aggregates. However, the height of electrostatic repulsion barrier gradually decreases with the increasing por-

porphyrin concentration, allowing formation of the small Ag colloidal aggregates for CuTMPyP(4) concentrations of  $(1-2) \times 10^{-7}$  M. Apparently, these small aggregates (30–70 particles) still carry residual charges, which prevent them from forming large aggregates ( $>100$  particles). The presence of these residual charges is well explained by the results of our experiments and calculation of the surface coverage which show that even the  $2 \times 10^{-7}$  M concentration (highest value of the SERRS intensity in the linear part of the concentration dependence) is sufficient only for a sub-monolayer coverage of Ag colloidal particles at which the negative charge of the residual ions is not fully compensated.

Finally, it has to be emphasized that the success of our SERRS spectral studies with nonaggregated Ag colloids was made possible by the proper choice of excitation wavelength. In the case of Ag colloid/CuTMPyP(4) systems, the 441.6 nm excitation line falls not only within the slope of the SPA band of isolated Ag colloidal particles (Figure 1a,e) but also within the slope of the Soret band of CuTMPyP(4) (maximum at 424 nm) (Figure 1). Both of these factors thus contribute to the advantage of the 441.6 nm excitation over the 514.5 nm excitation, for which the SERRS spectra of CuTMPyP(4) from systems with nonaggregated colloid were not obtained. Moreover, with 441.6 nm excitation, the OH stretching bands of bulk water are sufficiently strong to be observed in the SERRS spectra, allowing them to be employed as an internal intensity standard.

**5. Nonlinear Part of the Concentration Dependence of the SERRS Intensity: SERRS on Aggregated Ag Colloidal Particles.** To account for deviation of the SERRS signal from linear concentration dependence, observed for the systems with CuTMPyP(4) concentration  $\geq 3 \times 10^{-7}$  M (Figure 6) consisting of large aggregates of porphyrin-covered Ag colloidal particles (Figure 2a), as well as for the observed dependence of the decrease of the SERRS signal with an increasing porphyrin concentration on the frequency values of the individual vibrational modes (Figure 7), we have to consider the factors for which these systems differ from the systems with porphyrin concentration  $\leq 2 \times 10^{-7}$  M, providing the linear concentration dependence of the SERRS signal.

1. For  $3 \times 10^{-7}$  M concentration of CuTMPyP(4) in the system, nearly all porphyrin molecules introduced into the system are adsorbed on the colloidal particles. For this amount of adsorbed porphyrin molecules, the electrostatic repulsion barrier is, apparently, low enough to allow formation of large colloidal aggregates (Figure 2a). This fact manifests itself in a radical change of the shape of the SPA band (curve b in comparison to curve c, Figure 1). The relative increase of the SPA on curve b in comparison to curve c, is, apparently, an increasing function of the wavelength in the 450–480 nm range, which corresponds (for excitation 441.6 nm) to the wavelengths of the photons scattered by porphyrin vibrations. It means that for the aggregated Ag colloidal system and the excitation 441.6 nm higher surface enhancement of the Stokes Raman-scattered photons should be experienced by the high-frequency vibrational modes (with longer wavelengths of the Raman-scattered photons) than for the low-frequency modes. While this effect could explain the differences among the SERRS intensity versus concentration plots of the individual porphyrin modes occurring for concentrations  $\geq 3 \times 10^{-7}$  M, it cannot account for the overall decrease of the SERRS signal itself, since, in general, a greater SERRS enhancement of the Stokes Raman-scattered photons would be expected for the systems with large colloidal aggregates.

2. For the  $3 \times 10^{-7}$  M concentration, at which the radical change in the SERRS response of the system occurs, the amount

of porphyrin molecules present in the system is still somewhat lower than that required for a monolayer coverage. Since the depolarization effect of the neighboring molecules causing a break of the linear dependence of the SERS signal on surface coverage similar to that observed in the plots in Figure 6 was reported to occur at sub-monolayer surface coverage (close to two-thirds of a full monolayer coverage or lower) for cyanide anions adsorbed on Ag island films,<sup>20</sup> we find it necessary to consider this effect also in our case. Our system, however, differs from that described in ref 20 in several aspects: (1) in contrast to cyanide, porphyrin represents a multimode vibrational system, (2) the morphology of Ag colloids undergoes a substantially larger and “abrupt” change with increasing surface coverage than that of the island films, (3) the SERRS of the porphyrin is observed, in contrast to the SERS of cyanide, (4) the deviation from the linear concentration dependence appears at a substantially larger (but still sub-monolayer) coverage.

Considering also the specificity of the particular cationic porphyrin adsorbate, we suggest that the “depolarization effect” may have a rather specific form in our case, for which we propose the following model: Electrostatic repulsion between the (+4) charged CuTMPyP(4) molecules prevents formation of the porphyrin dimers in solution.<sup>13</sup> However, the situation is different for adsorbed CuTMPyP(4) molecules since their charges are compensated by anions covering the surface of Ag colloidal particles. Compensation of the charges on the colloidal surface is well demonstrated by aggregation of colloidal particles into large aggregates. Considering the size of the CuTMPyP(4) molecule in comparison to that of a Ag particle, as well as the fact that Ag particles bearing porphyrin molecules are brought together closely in the large colloidal aggregates, we can assume a rather strong interaction between the porphyrin molecules adsorbed on the neighboring colloidal particles. This interaction may well mimic formation of the porphyrin dimers. The results obtained for structurally related cationic porphyrins show that formation of dimers causes a blue shift of the Soret band and a decrease of its intensity to nearly half of its original value.<sup>21,22</sup> Both factors will induce a substantial decrease of the resonance enhancement of Raman scattering and, consequently, of the overall SERRS signal of the porphyrin upon 441.6 nm excitation. However, the described effect is an electronic effect that is supposed to affect all the resonance-enhanced modes in the same manner and does not account for the differences among the plots obtained in Figure 6 for the individual vibrational modes. Nevertheless, this model can well explain why the deviation of the plots from linearity occurs exactly at the same CuTMPyP(4) concentration as formation of large colloidal aggregates.

3. In systems with total porphyrin concentration  $> 3 \times 10^{-7}$  M, only a fraction of the total amount of porphyrin molecules introduced into the systems is adsorbed on Ag colloidal particles, as described quantitatively in Figure 3. However, the amount of adsorbed porphyrin molecules is a weakly increasing function of the total porphyrin concentration in the  $3 \times 10^{-7}$  to  $1 \times 10^{-6}$  M range. This factor itself thus cannot account for the constant and/or decreasing SERRS signal. However, the increasing concentration of the nonadsorbed porphyrin molecules can substantially increase absorption of both the incident and Raman-scattered radiation in the SERRS experiment. While absorption of the incident radiation affects the intensity of SERRS signal from all the porphyrin modes in the same manner, absorption of the scattered light is wavelength-dependent. Since the Soret absorption band of the CuTMPyP(4) decreases toward the red spectral region, the intensities of the high-frequency modes (with longer wavelengths of Stokes Raman-scattered

photons) will be less affected by reabsorption than those of the low-frequency ones. The increasing absorption of both the incident and Raman-scattered radiation will thus decrease the SERRS spectral intensity of the porphyrin spectral bands selectively in the order of their decreasing wavenumbers, as demonstrated in Figure 7.

In summation, our results indicate that the deviations from the linear concentration dependence of the SERRS spectral intensity of the  $A_{1g}$  porphyrin modes and their dependence on the mode frequency result from an interplay of several factors, the most important of which are the specific depolarization effect, the change of the SPA curve, and the increasing absorption of both the incident and the Raman-scattered radiation. Obviously, systems with porphyrin concentrations  $\geq 3 \times 10^{-7}$  M are not suitable for a quantitative SERRS spectral analysis.

## Conclusions

1. SERRS spectra of CuTMPyP(4) adsorbed on Ag colloidal particles excited by the 441.6 nm line of a He–Cd laser can be obtained for a wide range of total porphyrin concentrations ( $1 \times 10^{-9}$  to  $1 \times 10^{-6}$  M).

2. The OH stretching bands of bulk water can be used as an internal intensity standard to normalize the SERRS spectra.

3. The Ag colloid/CuTMPyP(4) system provides a unique opportunity to follow and mutually compare the concentration dependencies of (a) the SERRS signal of the adsorbate, (b) the surface coverage of Ag colloidal particles by the adsorbate molecules, (c) the morphology of the SERS-active system (isolated Ag colloidal particles and/or their aggregates), and (d) the SPA of the SERS-active system.

4. SERRS signal from systems with nonaggregated Ag colloidal particles and/or small colloidal aggregates (30–70 particles) is a linear function of the total porphyrin concentration in the system, which ranges from  $1 \times 10^{-8}$  to  $2 \times 10^{-7}$  M. This fact together with the long-term reproducibility of the SERRS spectra proves the suitability of these systems for quantitative SERRS spectral studies. By contrast, the systems with large colloidal aggregates and total porphyrin concentrations  $\geq 3 \times 10^{-7}$  M provide a highly nonlinear SERRS spectral response that varies with the particular vibrational mode frequency.

**Acknowledgment.** We thank Dr. Pavel Anzenbacher from the Institute of Organic Chemistry and Biochemistry, Prague,

for the preparation of the CuTMPyP(4) and Ms. Jiřina Hromádková from the Institute of Macromolecular Chemistry, Prague, for technical assistance with acquisition of TEM images. We thank Prof. Martin Moskovits, University of Toronto, and Dr. Laurent Chinsky from Université Pierre et Marie Curie, Paris, for valuable discussions. M.P. and P.M. gratefully acknowledge the French government for grants supporting their stays at L.P.B.C. This work was partially supported by the Grant Agency of Czech Republic (Grants 203/93/0106 and 203/97/0259) and the Grant Agency of Charles University (GAUK 96/219).

## References and Notes

- (1) Moskovits, M. *J. Chem. Phys.* **1978**, *69*, 4159.
- (2) Creighton, J. A.; Blatchford, C. G.; Albrecht, M. G. *J. Chem. Soc., Faraday Trans. 2* **1979**, *75*, 790.
- (3) Wetzel, H.; Gerischer, H. *Chem. Phys. Lett.* **1980**, *76*, 460.
- (4) Abe, H.; Manzel, K.; Schulze, W.; Moskovits, M.; DiLella, D. P. *J. Chem. Phys.* **1981**, *74*, 792.
- (5) Garrell, R. L.; Shaw, K. D.; Krimm, S. *Surf. Sci.* **1983**, *124*, 613.
- (6) Creighton, J. A. In *Surface Enhanced Raman Scattering*; Chang, R. K., Furtak, T. E., Eds.; Plenum Press: New York, 1982; p 315.
- (7) Moskovits, M. *Rev. Mod. Phys.* **1985**, *57*, 3.
- (8) Stockman, M. I.; Shalaev, V. M.; Moskovits, M.; Botet, R.; George, T. F. *Phys. Rev.* **1992**, *46*, 2821.
- (9) Heard, S. M.; Grieser, F.; Barraclough, C. G. *J. Colloid Interface Sci.* **1983**, *93*, 545.
- (10) Weitz, D. A.; Lin, M. Y.; Sandroff, C. J. *Surf. Sci.* **1985**, *158*, 147.
- (11) (a) Heard, S. M.; Grieser, F.; Barraclough, C. G. *Chem. Phys. Lett.* **1983**, *95*, 154. (b) Laserna, J. J.; Torres, E. L.; Winefordner, J. D. *Anal. Chim. Acta* **1987**, *200*, 469. (c) Vlčková, B.; Matějka, P.; Šimonová, J.; Čermáková, K.; Pančoška, P.; Baumruk, V. *J. Phys. Chem.* **1993**, *97*, 9719.
- (12) Čermáková, K.; Šesták, O.; Matějka, P.; Baumruk, V.; Vlčková, B. *Collect. Czech. Commun.* **1993**, *58*, 2682.
- (13) Pasternack, R. F.; Gibbs, E. J.; Villafranca, J. J. *Biochemistry* **1983**, *22*, 2406.
- (14) Sánchez-Cortés, J.; García-Ramos, J. V.; Morcillo, G. *J. Colloid Interface Sci.* **1994**, *167*, 428.
- (15) (a) Itoh, C.; Sugii, T.; Kim, M. *J. Phys. Chem.* **1988**, *92*, 1568. (b) Procházka, M. MSc. Thesis, Charles University, Prague 1994. (c) Matějka, P.; Mojžeš, P.; Vlčková, B. *J. Mol. Struct.* **1995**, *349*, 121.
- (16) Weitz, D. A.; Garoff, S.; Gersten, J. I.; Nitzan, A. *J. Chem. Phys.* **1983**, *78*, 5324.
- (17) Itoh, C.; Sugii, T.; Kim, M. *J. Phys. Chem.* **1988**, *92*, 1568.
- (18) Blom, N.; Odo, J.; Nakamoto, K.; Strommen, D. P. *J. Phys. Chem.* **1986**, *90*, 2847.
- (19) (a) Rowe, J. E.; Shank, C. V.; Zwemer, D. A.; Murray, C. A. *Phys. Rev. Lett.* **1980**, *44*, 1770. (b) Pockrand, I.; Otto, A. *Solid State Commun.* **1980**, *35*, 861. (c) Eesley, G. L. *Phys. Lett.* **1981**, *81A*, 193. (d) Pockrand, I. *Surf. Sci.* **1983**, *126*, 192.
- (20) Murray, C. A.; Bodoff, S. *Phys. Rev. Lett.* **1984**, *52*, 2273; *Phys. Rev. B* **1985**, *32*, 671.
- (21) Kano, K.; Takei, M.; Hashimoto, S. *J. Phys. Chem.* **1990**, *94*, 2181.
- (22) Bütje, K.; Nakamoto, K. *Inorg. Chim. Acta* **1990**, *167*, 97.